

# A decisive function of transforming growth factor- $\beta$ /Smad signaling in tissue morphogenesis and differentiation of human HaCaT keratinocytes

Susanne Buschke<sup>a,\*</sup>, Hans-Jürgen Stark<sup>a,\*</sup>, Ana Cerezo<sup>b</sup>, Silke Prätzel-Wunder<sup>a</sup>, Karsten Boehnke<sup>a</sup>, Jasmin Kollar<sup>a</sup>, Lutz Langbein<sup>a</sup>, Carl-Henrik Heldin<sup>c</sup>, and Petra Boukamp<sup>a</sup>

<sup>a</sup>Division of Genetics of Skin Carcinogenesis, Deutsches Krebsforschungszentrum (DKFZ), D-69120 Heidelberg, Germany; <sup>b</sup>Centro Nacional de Investigaciones Cardiovasculares (CNIC), 28029 Madrid, Spain; <sup>c</sup>Ludwig Institute for Cancer Research, Uppsala University, SE751 24 Uppsala, Sweden

**ABSTRACT** The mechanism by which transforming growth factor- $\beta$  (TGF $\beta$ ) regulates differentiation in human epidermal keratinocytes is still poorly understood. To assess the role of Smad signaling, we engineered human HaCaT keratinocytes either expressing small interfering RNA against Smads2, 3, and 4 or overexpressing Smad7 and verified impaired Smad signaling as decreased Smad phosphorylation, aberrant nuclear translocation, and altered target gene expression. Besides abrogation of TGF $\beta$ -dependent growth inhibition in conventional cultures, epidermal morphogenesis and differentiation in organotypic cultures were disturbed, resulting in altered tissue homeostasis with suprabasal proliferation and hyperplasia upon TGF $\beta$  treatment. Neutralizing antibodies against TGF $\beta$ , similar to blocking the actions of EGF-receptor or keratinocyte growth factor, caused significant growth reduction of Smad7-overexpressing cells, thereby demonstrating that epithelial hyperplasia was attributed to TGF $\beta$ -induced “dermis”-derived growth promoting factors. Furthermore impaired Smad signaling not only blocked the epidermal differentiation process or caused epidermal-to-mesenchymal transition but induced a switch to a complex alternative differentiation program, best characterized as mucous/intestinal-type epithelial differentiation. As the same alternative phenotype evolved from both modes of Smad-pathway interference, and reduction of Smad7-overexpression caused reversion to epidermal differentiation, our data suggest that functional TGF $\beta$ /Smad signaling, besides regulating epidermal tissue homeostasis, is not only essential for terminal epidermal differentiation but crucial in programming different epithelial differentiation routes.

## Monitoring Editor

Kunxin Luo  
University of California,  
Berkeley

Received: Nov 4, 2010

Revised: Jan 12, 2011

Accepted: Jan 18, 2011

This article was published online ahead of print in MBoC in Press (<http://www.molbiolcell.org/cgi/doi/10.1091/mbc.E10-11-0879>) on February 2, 2011.

\*These authors contributed equally to this work.

Address correspondence to: Petra Boukamp (P.Boukamp@dkfz-heidelberg.de).

Abbreviations used: BM, basement membrane; Dsg, desmoglein; ECM, extracellular matrix; EGFR, epidermal growth factor receptor; EMT, epithelial-mesenchymal transition; Gcnt3, glucosaminyl (N-acetyl) transferase 3, mucin type; IFE, interfollicular epidermis; IKK $\alpha$ , inhibitor of nuclear factor kappa-B kinase subunit  $\alpha$ ; KGF, keratinocyte growth factor; Klf4, Krueppel-like factor 4; OTC, organotypic culture; PAS, Periodic acid-Schiff; TGF $\beta$ , transforming growth factor- $\beta$

© 2011 Buschke et al. This article is distributed by The American Society for Cell Biology under license from the author(s). Two months after publication it is available to the public under an Attribution-Noncommercial-Share Alike 3.0 Unported Creative Commons License (<http://creativecommons.org/licenses/by-nc-sa/3.0>).

“ASCB®,” “The American Society for Cell Biology®,” and “Molecular Biology of the Cell®” are registered trademarks of The American Society of Cell Biology.

## INTRODUCTION

Skin, the largest organ of the human body, has an essential function as an inside/outside barrier. It is composed of two main tissue types: the epidermis constantly regenerated from keratinocytes and the dermis, an extracellular matrix (ECM) with fibroblasts providing the major cellular component. The two tissue types are separated by the basement membrane (BM), which also serves as an adherence structure for the epidermis. The basal layer of the epidermis mainly consists of epidermal stem cells and proliferative progenitor cells. The proliferating basal cells generate a suprabasal layer of nondividing cells that, upon further stratification, undergo a sequential program of differentiation, terminating in dead horn squames that are continually shed from the outer

surface. To maintain this homeostasis, proliferation and differentiation must be perfectly balanced. Although markers defining the different stages of human epidermal differentiation are already well described, the regulatory mechanisms underlying that process are still poorly understood.

It is widely documented that this regulation not only is an intrinsic trait of the epidermis itself but depends on an active paracrine interaction with its dermal microenvironment, providing growth factors and signals that facilitate epidermal stem cell maintenance, regeneration, and differentiation (Maas-Szabowski *et al.*, 2000; Szabowski *et al.*, 2000; Boehnke *et al.*, 2007). The transforming growth factor- $\beta$  (TGF $\beta$ ) is well implicated in this scenario by its dual function as inhibitor of epithelial cell growth and activator of fibroblast proliferation and protein synthesis. Thus TGF $\beta$  is involved in controlling the composition of the ECM and the epithelial microenvironment, including the epidermal stem cell niche. Accordingly, it was recently shown that the TGF $\beta$  family members not only are important regulators of stem cell renewal and differentiation, but they also contribute to tissue patterning (De Robertis and Kuroda, 2004; Watabe and Miyazono, 2009).

TGF $\beta$ -signals are perceived by cells through heteromeric complexes of two Type I and two Type II TGF $\beta$  receptors, both of which are transmembrane serine/threonine kinases. Downstream signaling is mediated by Smad molecules as well as other pathways, such as Erk, c-jun-N-terminal kinase, p38 mitogen-activated protein kinase, and phosphatidylinositol-3' kinase pathways (for a review, see Moustakas and Heldin, 2009). The canonical TGF $\beta$ /Smad pathway comprises phosphorylation and thereby activation of Smad2 and Smad3, forming complexes with Smad4 that are translocated into the nucleus to regulate transcription of TGF $\beta$ -responsive genes. Signal transduction is antagonized by the endogenous inhibitor Smad7, a target gene of Smad signaling that functions in a negative feedback loop.

TGF $\beta$  and its canonical Smad pathway have been studied in a number of mouse models, demonstrating their important role in skin development. Generally, interferences with the Smad pathway resulted in hair follicle phenotypes while the interfollicular epidermis (IFE) remained largely unaffected (Owens *et al.*, 2008). In human skin, hair follicles are generally rare, and a multilayered IFE prevails. Thus it remains elusive how abrogation of Smad pathway regulation would interfere with the differentiation process of the IFE in human skin. To better understand TGF $\beta$ /Smad regulation in human keratinocytes, many studies were performed in conventional two-dimensional (2D)-monolayer cultures using immortalized human HaCaT skin keratinocytes as an accepted model, which allowed deeper insights into the regulation of TGF $\beta$ -dependent Smad signaling and distinct functional consequences *in vitro* (for a review, see Brown *et al.*, 2007). Its impact on tissue organization and proper epidermal differentiation could not be addressed, however, due to the lack of appropriate human three-dimensional (3D) skin models. We recently demonstrated the significance of 3D organotypic cultures (OTCs) for epidermal stem cell growth and differentiation (Stark *et al.*, 2004, 2006; Muffler *et al.*, 2008) and used these OTCs here to investigate the role of TGF $\beta$ /Smad signaling in the process of human epidermal growth and differentiation.

By interfering with the TGF $\beta$  pathway at different nodes and analyzing the resulting effects on tissue formation, we could uncover decisive functions of canonical Smad signaling in the regulation of human epidermal differentiation and provide new major insights into TGF $\beta$ /Smad signaling as a key regulator of alternative epithelial differentiation programs.

## RESULTS

### Two modes to interfere with TGF $\beta$ -dependent growth inhibition

The central role of the Smad pathway in TGF $\beta$ -mediated signaling prompted us to investigate two HaCaT variants genetically engineered to intervene at different points with this pathway: H-S234KD cells transfected with a single RNA interference vector simultaneously targeting Smad2, Smad3, and Smad4 (Jazag *et al.*, 2005), and H-Smad7 cells selected for strong and stable expression of the inhibitory Smad7 (Supplemental Figure S1).

When measuring growth kinetics upon TGF $\beta$ -treatment (5 ng/ml), the parental HaCaT cells rapidly underwent growth arrest, whereas the genetically engineered cell lines continued to proliferate (Supplemental Figure S2). Interestingly, both cell lines exhibited accelerated growth in the absence of TGF $\beta$ , and even upon TGF $\beta$  treatment the growth rates did not fall below that of untreated parental HaCaT cells.

### Both HaCaT variants show different responses in the canonical Smad pathway

To characterize the effects of distinct interferences on TGF $\beta$  signaling, we investigated the response profiles of the canonical Smad pathway. As expected, TGF $\beta$  caused rapid phosphorylation of Smad2 and Smad3 at the expense of total Smad protein in the TGF $\beta$ -sensitive control HaCaT cells. In H-S234KD cells, phosphorylation of Smad2 was minimal, and Smad3 phosphorylation occurred only later (Figure 1A). The Smad3 level being generally low may suggest that TGF $\beta$  treatment actually induced *de novo* expression of Smad3. Indeed, when measuring Smad3 RNA expression, real-time PCR revealed a steady increase in HaCaT cells and a clear increase in H-S234KD cells after 24 h (Figure 1B). In H-Smad7 cells, transient phosphorylation of Smad2 and continuous phosphorylation of Smad3 were induced in response to TGF $\beta$ , whereas Smad3 RNA expression remained largely unchanged for up to 72 h (Figure 1, A and B).

To be functionally active, the phosphorylated Smad proteins require translocation into the nucleus (Inman *et al.*, 2002). Therefore we determined the subcellular localization of Smad2 and Smad3 before and after 90 min of TGF $\beta$  treatment (Figure 2). Before TGF $\beta$  treatment, all cells showed some cytoplasmic localization of Smad2 and Smad3, although the number of positive cells and the staining intensity varied (Figure 2, A, A'-C, and C'). On TGF $\beta$  treatment, nuclear translocation of Smad2 and Smad3 occurred in 100% of the parental HaCaT cells (Figure 2, D and D') and in ~25% of the H-S234KD cells (Figure 2, E and E'), suggesting that this subfraction of cells may express residual amounts of Smads, responsible for the Smad phosphorylation seen in the Western blots (see Figure 1A). In cultures of Smad7 cells, all of the nuclei were positively stained, albeit at a low level (Figure 2, F and F').

As these findings argued for some Smad pathway activation also in the HaCaT variants, we analyzed the expression patterns of known target genes (*i.e.*, cyclin-dependent kinase inhibitors p15<sup>INK4B</sup> [hereafter p15], p21<sup>WAF1/Cip1</sup> [hereafter p21], and plasminogen activator inhibitor type 1 [PAI-1]) (Dennler *et al.*, 1998; Song *et al.*, 1998; Hua *et al.*, 1999; Datta *et al.*, 2000; Providence *et al.*, 2000) (Figure 1A). While in control HaCaT cells, the level of all three proteins was strongly induced within 6 h of TGF $\beta$  treatment, H-S234KD cells showed a temporary induction of p21 and PAI at 6 h and a continuous increase of p15 expression. Otherwise, H-Smad7 cells showed an induction of p21 and, to a lesser extent, of PAI-1, whereas p15 remained suppressed. Thus neither of the two HaCaT variants became fully unresponsive to TGF $\beta$ , but the canonical Smad pathway

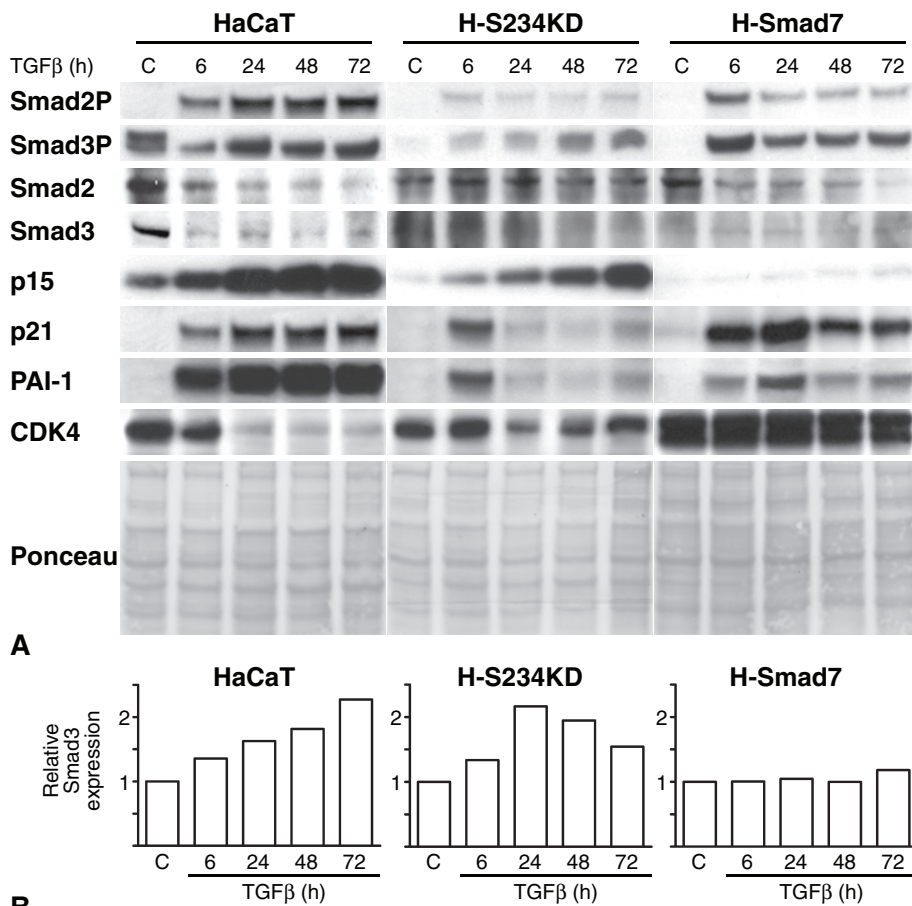


**FIGURE 1:** Interference with TGFβ/Smad pathway causes diverse molecular responses. (A) Western blot analyses from untreated and TGFβ-treated lysates from HaCaT, H-S234KD, and H-Smad7 cells were performed to determine the degree of Smad2 and -3 phosphorylation and total nonphosphorylated Smad2 and -3 expression as well as the level of target gene—p15, p21, PAI-1, and CDK4—induction on 6, 24, 48, and 72 h of TGFβ treatment. Ponceau, staining for loading control. (B) qRT-PCR analysis of Smad3 RNA expression in HaCaT, H-S234KD, and H-Smad7 cells on 6, 24, 48, and 72 h of TGFβ treatment.

was clearly impaired in H-S234KD and H-Smad7 cells, although with different downstream consequences.

Halder *et al.* (Halder *et al.*, 2005) proposed a down-regulation of the cell-cycle activator CDK4 in response to TGFβ under contribution of Smad proteins. Indeed, CDK4 gene expression was completely inhibited by TGFβ in the parental HaCaT cells and remained unaltered in both variants (Figure 1A). In contrast, cyclin D1, the regulatory subunit of CDK4 (Hunter and Pines, 1994), even increased upon TGFβ treatment in the parental HaCaT cells as well as in the HaCaT variants (Supplemental Figure S3 and unpublished data), suggesting that CDK4, but not cyclin D1, is regulated in the TGFβ-dependent scenario.

### Interference with TGFβ/Smad signaling impairs tissue homeostasis and overcomes TGFβ-mediated growth arrest also in the *in vivo*-like OTCs

In skin, epidermal proliferation and morphogenesis are regulated by the mutual interaction of the epidermal keratinocytes with the dermal fibroblasts and/or the factors derived from these cells (Maas-Szabowski *et al.*, 1999; Boehnke *et al.*, 2007). In OTCs of human keratinocytes, this interplay is well recapitulated, and TGFβ can exert its opposed effect on the dermal fibroblasts, which, in contrast to keratinocytes, are stimulated to proliferate and to synthesize matrix

proteins (for a review, see Brown *et al.*, 2007). To evaluate the impact of Smad-pathway interference in this *in vivo*-like environment, we established OTCs with the different HaCaT variants. Without exogenous TGFβ, parental HaCaT cells formed a stratified, well-differentiated, epidermis-like epithelium with few proliferating cells in the basal compartment (Figure 3A). On TGFβ treatment, HaCaT cells were significantly growth inhibited despite the fact that the number of fibroblasts was significantly increased (Figure 3A), confirming their sensitivity to TGFβ also in the “*in vivo*” situation. Different from the parental cells, the HaCaT variants formed stratified epithelia that were altered in cell morphology and histology. Moreover, they showed increased proliferation in the absence of exogenous TGFβ (Figure 3, B and C). Most notably, proliferation was no longer restricted to the basal layer, indicating that impaired Smad signaling remarkably affected tissue homeostasis. Exposure to TGFβ did not result in reduced epithelial proliferation (Figure 3, B' and C'), confirming that, also under these *in vivo*-like conditions, TGFβ-dependent growth inhibition was largely diminished.

### Abrogation of TGFβ-dependent growth inhibition does not impair sensitivity to other growth-stimulating factors

Different from monolayer cultures, with TGFβ treatment still causing some growth reduction (see Supplemental Figure S2), H-Smad7 cells responded to TGFβ with epithelial hyperplasia when grown in OTCs (see Figure 3C'). To determine whether this response was based on inherent properties or

was a result of extrinsic stimulation (i.e., paracrine interaction through growth factors provided by the TGFβ-stimulated dermal fibroblasts), H-Smad7 cells were first grown in the absence of fibroblasts. The developing epithelium consisted of only a few cell layers (Figure 4A), demonstrating that similar to normal keratinocytes and HaCaT cells (Boehnke *et al.*, 2007, and unpublished data), these cells still depended on the paracrine stimulation by fibroblast-derived factors for steady proliferation and formation of a stratified epithelium. With fibroblasts present, a multilayered epithelium was formed (Figure 4B), which, upon TGFβ treatment, became severely hyperplastic (Figure 4C).

To further determine the role of TGFβ in epithelial hyperplasia, we blocked its action in HaCaT and H-Smad7 OTCs by the addition of a neutralizing antibody (Figure 4, G–L). As expected, in HaCaT OTCs the TGFβ-dependent growth inhibitory effect was completely abolished, and the cells formed a well-stratified and differentiated epidermis-like epithelium (Figure 4, G and H), clearly demonstrating the efficacy of the neutralizing antibody. Also, without exogenous TGFβ, the addition of the neutralizing antibody allowed for the formation of a similar well-stratified and differentiated epithelium, suggesting that endogenous TGFβ was negligible for epidermal tissue morphogenesis (Figure 4I). Furthermore proliferation remained restricted to the basal layer (unpublished data). In H-Smad7 cultures,

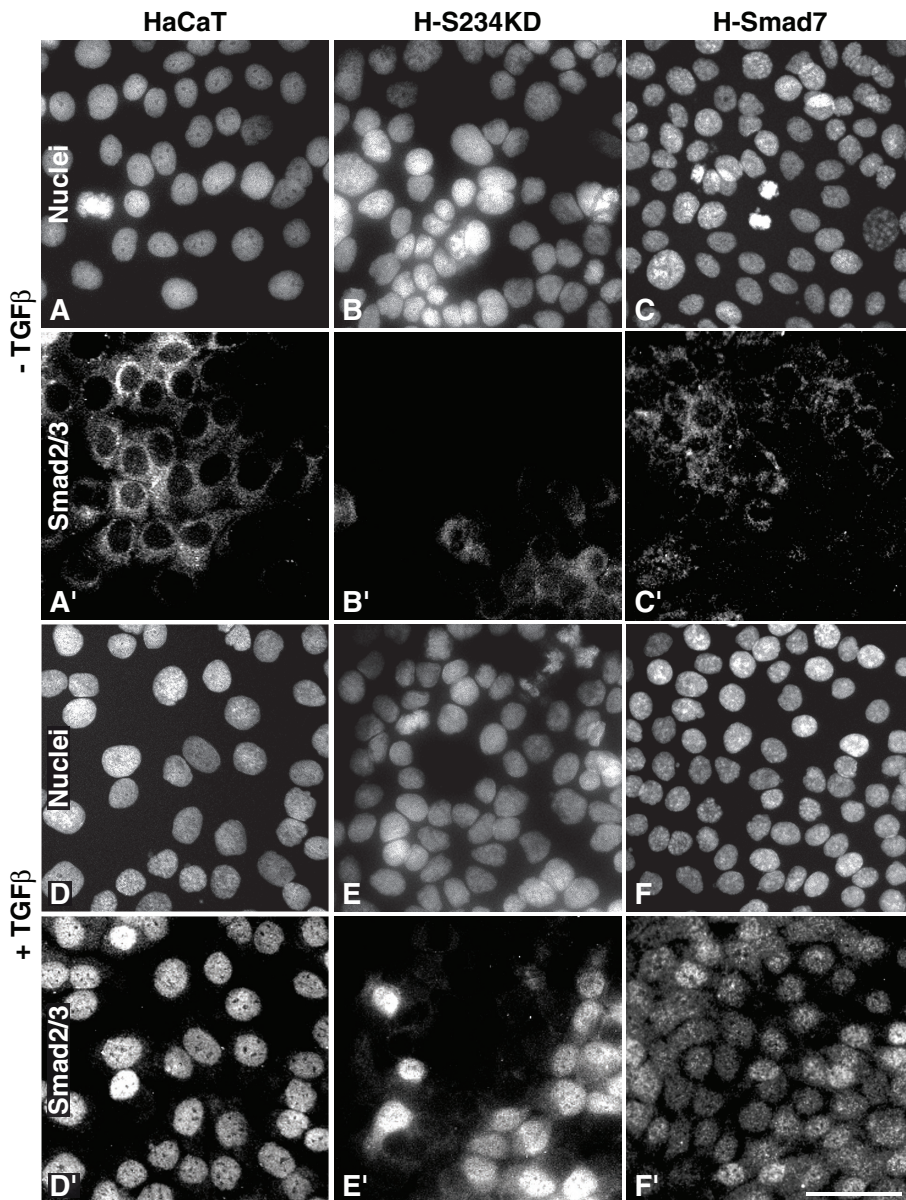


**FIGURE 2:** Nuclear translocation of Smad2/3 occurs in HaCaT cells and all variants upon TGF $\beta$  treatment. Immunofluorescence detection of Smad2 and -3 in HaCaT (A/A' and D/D'), H-S234KD (B/B' and E/E'), and H-Smad7 cells (C/C' and F/F') before and after a 90-min treatment with TGF $\beta$  (5 ng/ml). Nuclei, Hoechst counterstain. Bar = 50  $\mu$ m.

in contrast, the TGF $\beta$ -neutralizing antibody prevented hyperplasia (Figure 4, J and K), and the thickness of the epithelium was similar to that of H-Smad7 control cultures or cultures treated only with the neutralizing antibody (Figure 4L and unpublished data).

As EGF and the mesenchyme-derived keratinocyte growth factor (KGF) are major keratinocyte mitogens (Shirakata, 2010), we applied inhibitory antibodies against EGF receptor (EGFR) (in the presence of TGF $\beta$ ) to H-Smad7 cultures, and hyperplasia was consequently inhibited (Figure 4D). Furthermore neutralizing antibodies against KGF had an even stronger effect (Figure 4E) and, finally, a simultaneous inhibition of KGF and EGFR reduced stratification to the level seen in the absence of fibroblasts (Figure 4F). The addition of an isotypic control antibody against an irrelevant epitope (pox virus protein) had no effect on the growth of the H-Smad7 cells (unpublished data). Together these results confirmed the important role of TGF $\beta$  in inducing EGF and KGF as crucial paracrine growth regulators

for epithelial cell hyperplasia and illustrate the importance of TGF $\beta$  signaling as a counterbalancing negative control to achieve tissue homeostasis.

### Attenuated TGF $\beta$ /Smad signaling entails altered epidermal morphogenesis and differentiation in OTCs

Interference with TGF $\beta$ /Smad pathway regulation led to modulated proliferation and distinct alterations in tissue morphology. Only the parental HaCaT cells developed a regular, well-organized parakeratotic epidermis-like epithelium (Figure 5A). H-S234KD and H-Smad7 epithelia had largely lost their epidermal architecture. They were composed of rather uniform small cells and contained either sporadically (H-S234KD epithelia) or frequently (H-Smad7 epithelia) balloon-like cavities (Figure 5, B and C). Both number and size of these cavities increased with time, suggesting that they reflected an inherent property of this alternative differentiation program.

On TGF $\beta$  treatment, which inhibited proliferation of the HaCaT cells as evident by reducing stratification to one to two layers of flat cells (Figure 5A'), epithelia of the two variants with impaired Smad signaling, the H-S234KD and H-Smad7-cells, stably maintained their non-epidermal phenotype as obvious in histology (Figure 5, B' and C').

To define the molecular basis of the changes, we first examined the expression of well-known protein markers for epithelial differentiation stages, including the intermediate filament keratin K5, the desmosomal components desmoplakin and desmoglein (Dsg)3, and the adherence junction molecule, E-cadherin, all of them orderly expressed and distributed in HaCaT epithelia (Supplemental Figure S4, A, D, G, and J). Also, in H-S234KD, epithelia expression and localization were largely unaltered. Otherwise, in H-Smad7 epithelia, these proteins

were expressed at reduced levels and with abnormal distributions (Supplemental Figure S4, B, E, H, K and C, F, I, L). In accordance with disturbed tissue homeostasis (i.e., proliferation throughout the epithelium), the  $\beta_1$  integrins as cell-matrix adhesion molecules and the hemidesmosomal component  $\alpha_6\beta_4$  integrin, normally restricted to the basal cells (see HaCaT epithelia, Supplemental Figure S4, M and P), were found throughout the entire epithelium in H-S234KD and H-Smad7 OTCs (Supplemental Figure S4, N, Q, and O, R). Vimentin, the typical intermediate filament protein of mesenchymal cells, was restricted to the fibroblasts of the dermal equivalents (Supplemental Figure S4, S–U). These findings provide evidence for the strictly maintained epithelial nature of the modified HaCaT cells without any sign of epithelial–mesenchymal transition (EMT) as a result of Smad pathway abrogation (for a review, see Heldin *et al.*, 2009).

With the onset of differentiation, HaCaT keratinocytes expressed the keratins K1 and K10 (Figure 6A), the cornified envelope protein

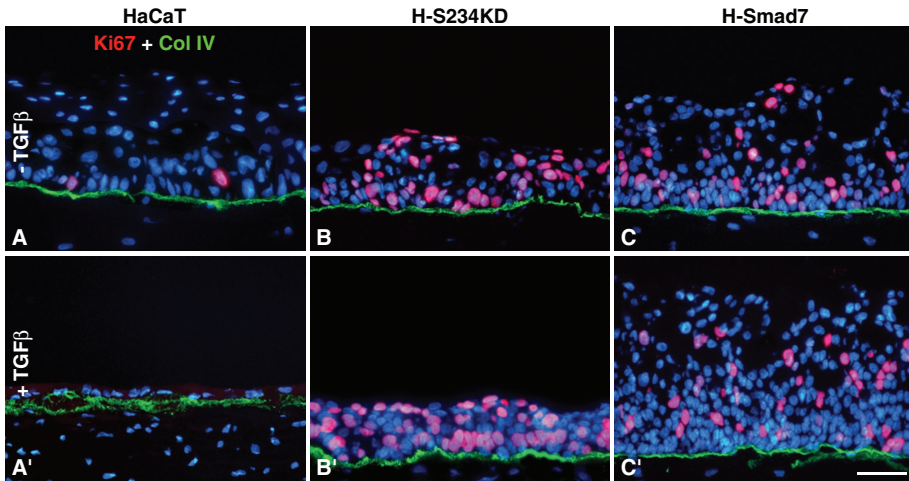


**FIGURE 3:** In OTC proliferation control by TGFβ1 is abrogated in the HaCaT variants. Immunofluorescence staining of 3-wk-old OTCs of HaCaT (A), HS234KD (B), and H-Smad7 (C) cells for proliferation (Ki67 in red) and collagen Type IV (col IV in green) to mark the BM separating the epithelium from the dermal compartment. (A–C), untreated cultures; (A'–C'), cultures treated with TGFβ. Note the increased number and the abnormal suprabasal distribution of Ki67-positive cells in the three variants. Nuclei, Hoechst counterstain.

involucrin (unpublished data), the epidermis-specific transglutaminase-1 (Figure 6D), and Dsg1 (Figure 6G), the major desmosomal cadherin in the suprabasal layers of the epidermis (Green and Simpson, 2007). This regular pattern was also found in H-S234KD epithelia (Figure 6, B and E) with the exception of Dsg1, which was strongly reduced (Figure 6H). H-Smad7 cells, in contrast, expressed little, if any, of the examined markers (Figure 6, C, F, and I). Although HaCaT epithelia realized advanced terminal epidermal differentiation as assessed by the expression of filaggrin, loricrin, keratin K2 (formerly K2e), and Dsg4 (Figure 6, J, M, and P, and unpublished data), these markers were largely absent in both variants (Figure 6, K, N, Q and L, O, R).

### Impaired TGFβ/Smad signaling in HaCaT keratinocytes induces an alternative differentiation program

The distinct and reproducible phenotype of the H-S234KD and H-Smad7 epithelia not only argued for a block within the epidermal differentiation program, but for a switch to an alternative differentiation route. As cornification was missing, a shift to a “mucous” noncornified squamous epithelium was most likely. Consistent with this hypothesis, the keratins K4 and K13, typical for differentiated layers of squamous epithelia (for a review, see Moll *et al.*, 2008) (Figure 7, A and D), were strongly increased and, as in those epithelia, extended throughout the suprabasal strata of both variants (Figure 7, B, E and C, F). Furthermore the simple-epithelial-type keratins—K7, K8, K18, and K19—expressed during embryonic development

of the epidermis and characteristic of non-stratified (e.g., intestinal) epithelia, were prominent throughout the epithelium in all HaCaT variants (Figure 7, G–L and unpublished data), arguing for a complex shift in the differentiation program.

To further characterize this particular differentiation program, we tested for cellular tight junctions that are typical for epithelia with pronounced barrier function and are located in upper living cells of the *stratum granulosum* of the epidermis as well as in glandular epithelia (Langbein *et al.*, 2002, 2003, and references therein). Both of the typical tight junction proteins, occludin and cingulin, appeared at the margins of the *granulosum*-like cells in parental HaCaT epithelia (Figure 7M and unpublished data). In H-S234KD and H-Smad7 epithelia, these proteins could also be attributed to the lining of the cavities, strongly resembling glandular structures (Figure 7, M inset, N, and O,

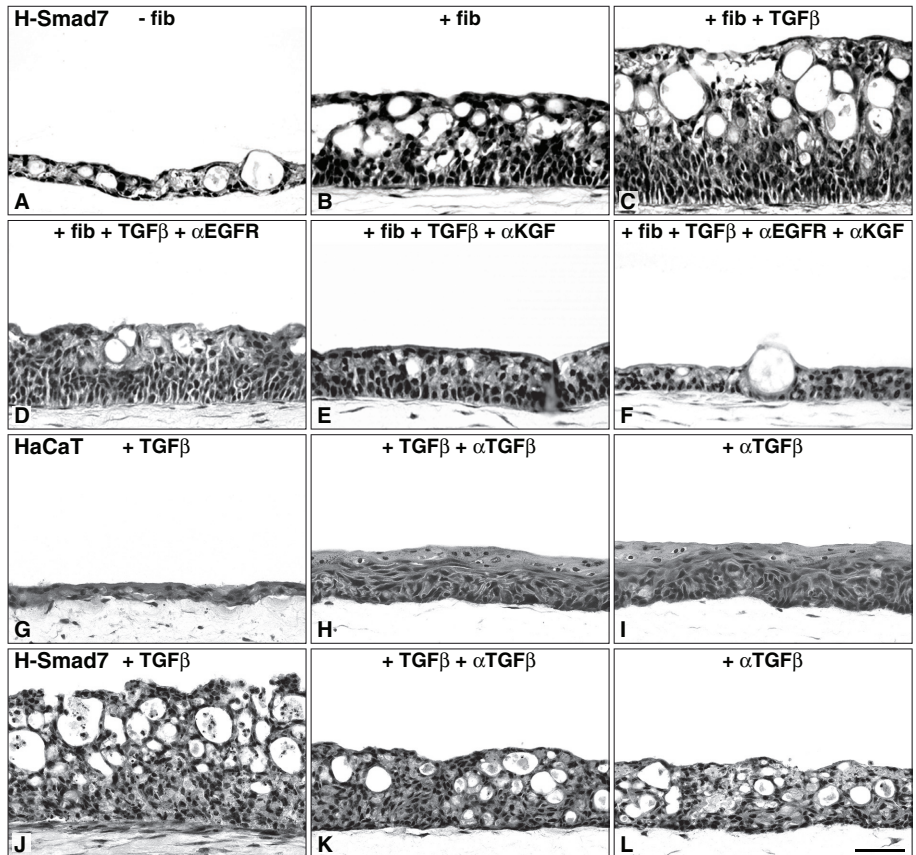


**FIGURE 4:** (A–F) Dependence on dermal fibroblasts and their growth factors is unaltered. Histological sections of H-Smad7 cells were grown in OTCs for 3 wk without fibroblasts (– fib) (A), with fibroblasts (+ fib) in the dermal equivalent (B), with fibroblasts in the presence of TGFβ (+ fib + TGFβ) (C), and on treatment with a neutralizing antibody against the EGFR (+ fib + TGFβ + αEGFR) (D), in the presence of TGFβ and a neutralizing antibody against KGF (+ fib + TGFβ + αKGF) (E), as well as addition of the two neutralizing antibodies against KGF and EGFR (+ fib + TGFβ + αKGF + αEGFR) (F). Histological sections of HaCaT (G–I) and H-Smad7 epithelia (J–L) grown in OTCs for 16 d and treated with TGFβ (G and J), TGFβ plus a neutralizing antibody against TGFβ (αTGFβ, H and K), and the neutralizing antibody against TGFβ only (I and L). Bar = 100 μm.

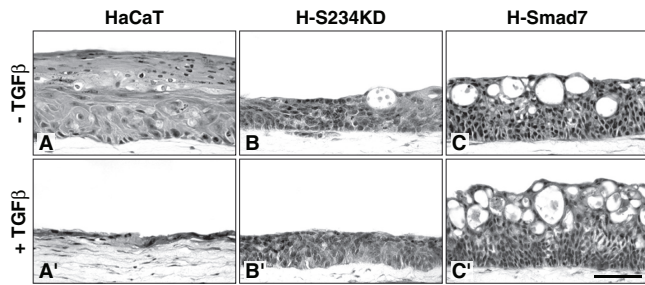


**FIGURE 5:** Abrogation of epidermal tissue morphology by impaired TGF $\beta$ /Smad signaling. Histological sections of 3-wk-old OTCs from HaCaT cells and the transgenic HaCaT variants untreated (A–C) and treated with TGF $\beta$  (A'–C'). (A) The parental HaCaT cells show a typical epidermis-like epithelium with a parakeratotic *stratum corneum*. (B) The H-S234KD epithelia are composed of uniform small cells regularly forming cavities in the upper part of the epithelium. (C) H-Smad7 cells form a similar non-epidermal-type epithelium, however, with an increased number of cavities. Upon TGF $\beta$  treatment, (A') HaCaT growth is restricted to only one to two cell layers of flat cells. (B') The morphology of H-S234KD is largely unchanged except that the number of cavities is reduced. (C') H-Smad7 cells have formed a non-epidermal-like hyperplastic epithelium with numerous cavities. Bar = 100  $\mu$ m.

and unpublished data). A gland-like differentiation was further supported by the expression of *Dsg2*, which is predominantly found in sweat gland acini of the skin (Figure 7, P inset, Q, and R, and Green and Simpson, 2007). A differentiation typical for sweat gland ductal epithelium, as defined by keratin 77 (formerly K1b) expression, in contrast, could be excluded (unpublished data). Using three different histochemical staining techniques—Periodic acid–Schiff (PAS), mucicarmine, and Alcian blue—the cavities in H-S234KD and H-Smad7 epithelia were identified as mucin-containing structures (Figure 8, A–D, and unpublished data). The biosynthesis of mucin could be confirmed by reverse transcription (RT)-PCR analysis detecting the expression of different mucins, such as mucins 4 and 13, but also of enzymes required for mucin synthesis and modification, such as glucosaminyl (N-acetyl) transferase 3, mucin type (*Gcnt3*) (Li *et al.*, 2009). The expression of mucin 13 and *Gcnt3* were less prominent in conventional monolayer cultures of H-S234KD and H-Smad7 cells, but intensified in OTCs (Figure 8E). Obviously, this alternative differentiation program required the tissue context for its optimal development. Furthermore the phenotypic differences between HaCaT cells and the two variants with impaired Smad signaling became even more pronounced in long-term OTCs (>8 wk). Whereas HaCaT cells regenerated an orthokeratinized epidermis, the epithelia of H-S234KD and H-Smad7 cells retained their alternative phenotype. Furthermore due to the high cellular turnover in H-Smad7 OTCs, accompanied by a steady rupturing of the cavities, increased secretion of mucus, as well as shedding of cellular material, the epithelial thickness became reduced and in 10-wk-old culture closely resembled thin glandular epithelia (Figure 8, F–H).

#### Loss of terminal epidermal differentiation correlates with loss of Krueppel-like factor 4

Functional impairment of the Smad pathway not only affected expression of single differentiation genes but blocked the entire process of epidermal differentiation. This finding suggests that this pathway plays a crucial role in the regulation of epidermal differentiation. Additional factors reported to be prerequisite for keratinocyte differentiation are inhibitor of nuclear factor kappa-B kinase

subunit  $\alpha$  (IKK $\alpha$ ) and the transcription factor Krueppel-like factor 4 (Klf4). IKK $\alpha$  was recently shown to be an important coregulator of a Smad4-independent TGF $\beta$ –Smad2/3 signaling pathway that controls keratinocyte differentiation (Descargues *et al.*, 2008). We found that IKK $\alpha$  was equally expressed both in the epithelia of the parental HaCaT cells and in the two genetic variants (Figure 9), suggesting that regulation via IKK $\alpha$  was not the predominant regulatory event underlying epidermal differentiation and that IKK $\alpha$  was not regulated in a Smad pathway–dependent manner.

As well, Klf4 has previously been shown to regulate the expression of a group of differentiation-specific epidermal keratins (Chen *et al.*, 2003) and to play an important role in controlling barrier function (Patel *et al.*, 1997). We found high Klf4 mRNA expression for the epidermal differentiation phenotype of the parental HaCaT cells whereas expression was strongly reduced concomitantly with the alternative differentiation phenotype in the epithelia of the H-234KD and H-Smad7 cells (Figure 9).

#### Smad pathway abrogation is causal for switching the epithelial differentiation phenotype

Despite the fact that some Smad pathway activation still occurred in both H-S234KD and H-Smad7 cells, the alternative differentiation phenotype was unaffected by treatment with TGF $\beta$  (see Figure 5, B' and C'). Furthermore Klf4, the crucial factor required for terminal epidermal differentiation, remained suppressed (Figure 9 and unpublished data). Therefore we asked whether reduction of the Smad7 level in H-Smad7 cells would allow for reversion to epidermal differentiation. To accomplish sufficient and long-lasting reduction, we treated H-Smad7 OTCs with control and Smad7 antisense oligonucleotides. The application of control oligonucleotides neither affected Smad7 expression nor altered the differentiation profile (Supplemental Figure S5A and Figure 10, A–D). Incubation with Smad7 antisense oligonucleotides, however, caused a significant reduction of Smad7 RNA expression (Supplemental Figure S5B). Concomitantly, markers characteristic for the alternative differentiation (e.g., keratin K7) (Figure 10A), were strongly down-regulated, whereas the epidermal differentiation markers, shown for involucrin (Figure 10B), became dominant. Even terminal differentiation markers such as filaggrin were reexpressed, although localized in a scattered pattern (Figure 10C). Along with decelerated proliferation, tissue homeostasis normalized, as suggested from the distribution of the  $\alpha_6$  and  $\beta_1$  integrin chains, which became restricted to the basal compartment of the epithelium (Figure 10D' and unpublished data). These results could be reproduced with a second set of Smad7 antisense oligonucleotides as well as with a different clone of H-Smad7 cells (unpublished data), thus confirming their general validity.

Collectively these observations strongly argue for the absolute necessity of an intact and active Smad pathway for the process of regular epidermal differentiation and for its role as a regulatory switch between different epithelial differentiation programs.

#### DISCUSSION

To study the role of TGF $\beta$ -Smad signaling in the growth and differentiation of human skin keratinocytes, we engineered HaCaT variants, H-S234KD and H-Smad7 cells, that showed impaired Smad signaling as verified by decreased Smad phosphorylation, nuclear translocation, and altered target gene expression profiles. As expected, these cells exhibited a distinct abrogation of the well-known TGF $\beta$ -dependent growth inhibition in conventional cultures and proved to be excellent tools to unravel how the Smad pathway contributes to growth and differentiation also under *in vivo*-like

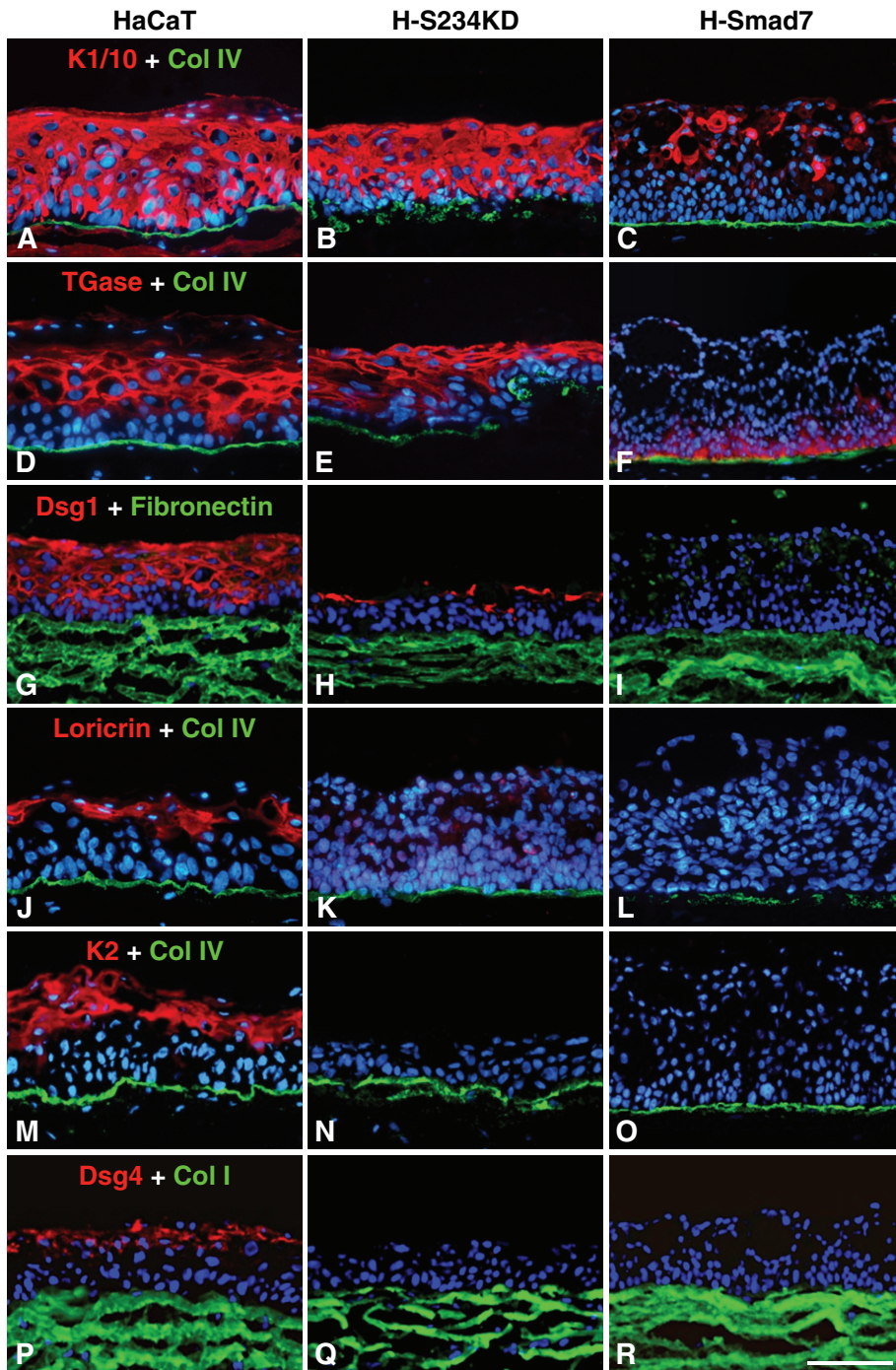


**FIGURE 6:** Alterations in epidermal differentiation on interference with TGF $\beta$ /Smad signaling. Immunofluorescence detection demonstrates a normal distribution of the epidermal differentiation markers keratin K1 and K10, transglutaminase 1, and Dsg1 in HaCaT (A, D, G). In H-S234KD epithelia K1/10 (B) and transglutaminase 1 (E) are normally expressed whereas Dsg1 is largely absent (H). In H-Smad7 epithelia, K1/10 (C) and transglutaminase 1 (F) are only faintly expressed or are lacking (Dsg1; I). The “late” differentiation markers loricrin, keratin K2, and Dsg4 (all in red) are restricted to the HaCaT epithelium (J, M, P), while being absent in the epithelia of H-S234KD (K, N, Q), and H-Smad7 cells (L, O, R). In (A–F) and (J–O), collagen Type IV (col IV) counterstaining is used to demarcate the BM separating the epithelium from the dermal equivalent, and the entire dermal matrix was stained with antisera against fibronectin (G–I) and collagen Type I (P–R). Nuclei, Hoechst counterstain. Bar = 100  $\mu$ m.

conditions (i.e., when propagated in OTCs). From these studies two major findings emerged. First, epidermal tissue homeostasis, closely linked to the epidermal differentiation process, required ac-

tive TGF $\beta$ /Smad signaling. Second, active Smad signaling was essential for terminal epidermal differentiation. Abrogation of the Smad signaling pathway not only blocked the epidermal differentiation process but induced a switch to a highly complex alternative differentiation program, suggesting that TGF $\beta$ /Smad signaling was responsible for programming different epithelial differentiation routes.

### Smad signaling regulates tissue homeostasis

So far, studies that address the role of TGF $\beta$ /Smad signaling in tissue regulation are restricted to mice. These studies showed that knockdown of Smad2 and Smad3 in the epidermis did not result in any obvious skin phenotype; however, Smad4 deletion resulted in hair follicle collapse. Whereas the triple knockdown of Smad2, -3, and -4 in keratinocytes was not yet reported, Smad7 overexpression showed the most distinct effects (reviewed in Owens *et al.*, 2008). These mice exhibited multiple developmental defects in the stratified epithelia, and, when using an inducible system for overexpressing Smad7 at different stages of development in the epithelial cells, Han and coworkers demonstrated a significant delay in embryonic hair follicle development and complete blockade of hair follicle differentiation. Actually, sebaceous gland development was significantly accelerated, and epidermal differentiation was perturbed (Han *et al.*, 2006). Furthermore these mice exhibited aberrant hair follicle cycling (Han *et al.*, 2006), suggesting a major disturbance in hair follicle homeostasis. In agreement with this finding, when performing H-Smad7 OTCs, the epithelia were not able to establish a stage of tissue homeostasis. Different from the epidermis of normal keratinocytes or HaCaT epithelia, where proliferation is restricted to the basal cell compartment and the integrin distribution is well organized, the Smad7-overexpressing H-Smad7 cells exhibited increased proliferation throughout all epithelial layers and, accordingly, an integrin profile similarly extending throughout the epithelium. As disturbance in tissue homeostasis remained unaffected by TGF $\beta$  treatment or long-term growth (>10 wk) in OTCs, and was similarly characteristic for the H-S234KD cells, these data strongly suggest that abrogation of Smad signaling was crucial for this abnormal growth behavior.

Different from the situation in monolayer cultures where TGF $\beta$  still caused some reduction in proliferation, the level of keratinocyte proliferation even increased upon TGF $\beta$  treatment when the HaCaT variants were cultivated in OTCs. In this tissue context, similar to that in skin, growth

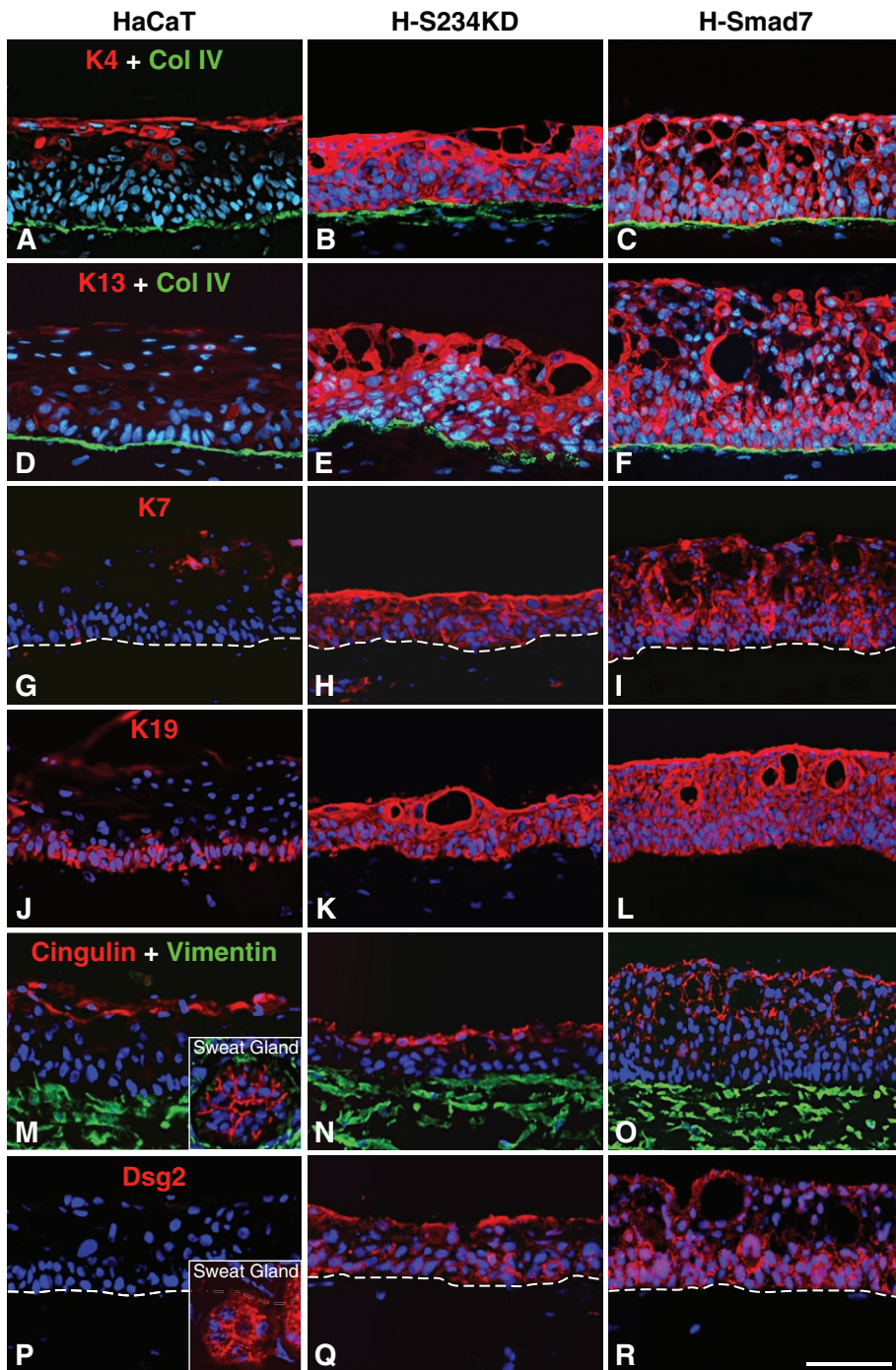


**FIGURE 7:** Induction of non-epidermal differentiation markers by impaired TGF $\beta$ /Smad signaling. Immunofluorescence detection in 3-wk-old OTCs from HaCaT cells and the two variants, H-S234KD and H-Smad7 cells, of the mucosal keratins K4 (A–C) and K13 (D–F), the “simple-type” intestinal keratins K7 (G–I) and K19 (J–L), and the tight junction protein cingulin (M–O, inset in M showing cingulin expression in human sweat gland) and Dsg2 (P–R, inset in P showing Dsg2 expression in human sweat gland). The marker proteins are shown in red and nuclei in blue. The BM is depicted by collagen IV staining (col IV in green, in A–F) and the fibroblast in the dermal equivalent with vimentin in (M–O). In (G–I) and (P–R) the BM is demarcated by dashed lines. Nuclei, Hoechst counterstain. Bars = 10  $\mu$ m (insets in M and P), 100  $\mu$ m (all other images).

factors are provided by the dermal fibroblasts that, in a paracrine regulation, are responsible for epidermal growth and differentiation (Contard *et al.*, 1993; Fusenig, 1994; Smola *et al.*, 1998; Szabowski *et al.*, 2000; El Ghalbzouri *et al.*, 2002). Accordingly, the severe hy-

perplasia of H-Smad7 epithelia, occurring upon TGF $\beta$  treatment in OTCs, could be ascribed to a still functional response to the growth-promoting factors provided by the dermal fibroblasts. Blocking the actions of EGFR or KGF caused reduction of hyperplastic growth, and the combined blockade of both confirmed that H-Smad7 cells depended on the growth-promoting action of the “dermis”-derived growth factors in the same way as the parental HaCaT cells or normal keratinocytes (Boehnke *et al.*, 2007). Thus abrogating the negative growth regulation by TGF $\beta$  resulted in an unrestricted response to keratinocyte mitogens and hyperplasia, further arguing for TGF $\beta$ /Smad signaling as being the crucial regulator counterbalancing growth promotion during epidermal tissue regeneration.

### Active Smad signaling is essential for terminal epidermal differentiation

Most importantly, impaired TGF $\beta$ /Smad signaling also caused a distinct differentiation phenotype. EMT, as a consequence of TGF $\beta$  action (for a review, see Heldin *et al.*, 2009) was not observed. The epithelial phenotype, evidenced by the expression of a large set of epithelial markers including E-cadherin and the lack of expression of the mesenchymal marker vimentin, was maintained in both variants. Thus EMT may not be a general response of HaCaT cells to TGF $\beta$ , but may require additional alterations in epithelial cells that occur during the process of tumorigenic transformation (e.g., H-ras activation), as recently proposed (Schafer and Werner, 2008). Consistently, none of the variants formed tumors when injected subcutaneously into nude mice (Boukamp, unpublished data). Instead, in OTCs, loss of epidermal differentiation was accompanied by a considerable decline in the expression of Klf4. This transcription factor has been shown to be essential for the formation of the epidermal barrier (Patel *et al.*, 1997) by regulating genes such as keratin K1, involucrin, or reptin and thereby contributing to a balanced cornified envelope assembly (Segre *et al.*, 1999). Actually, a 14-fold decline of Klf4 was first identified by RNA expression array analysis in conventional cultures of H-S234KD and H-Smad7 cells (unpublished data), and this strong reduction was confirmed in epithelia of both variants (Figure 9). In contrast, a third HaCaT variant being abrogated in TGF $\beta$ -dependent growth inhibition, but still exhibiting a fully functional TGF $\beta$ /Smad

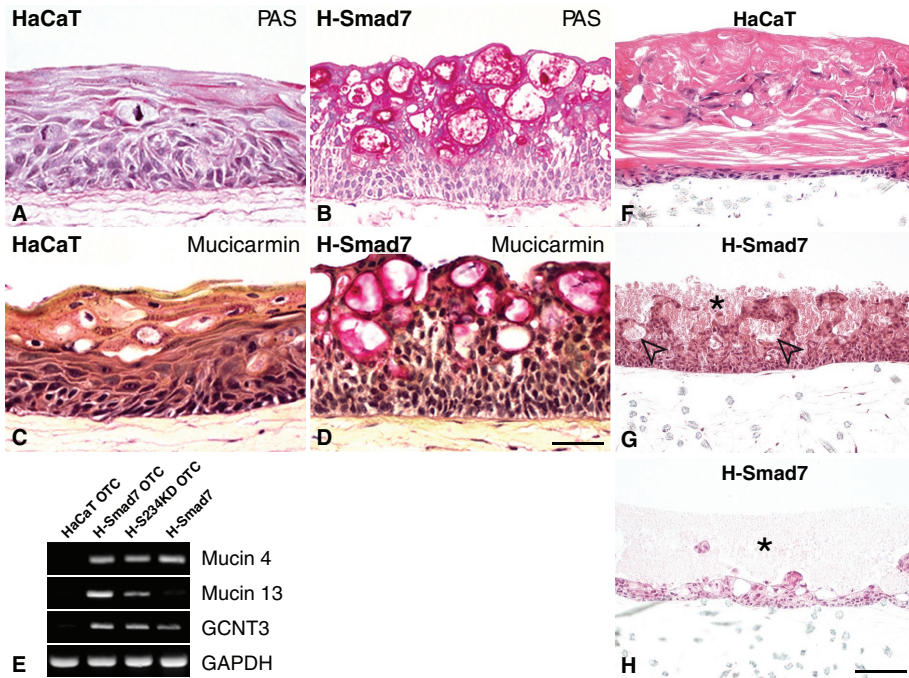


**FIGURE 8:** Mucin-containing cavities in H-Smad7 epithelia. Epithelia formed by HaCaT (A and C) and H-Smad7 cells (B and D) were stained by PAS and mucicarmin histochemistry. Note the red staining of the cavities, demonstrating mucin content, in H-Smad7 epithelia, whereas individual holes also found in HaCaT epithelia remain unstained. (E) mRNA expression of HaCaT, H-Smad7, and H-S234KD epithelia as well as H-S234KD cells from conventional cultures for mucins 4 and 13 and the *Gcmt3* involved in mucin biosynthesis. *GAPDH*, loading control. (F–H) Long-term OTCs of HaCaT and H-Smad7 cells. Whereas HaCaT cells form an orthokeratinized epidermis (F, 10-wk-old epithelium), H-Smad7 cells go through a phase of hyperplasia (G, 6-wk-old epithelium) and continuous release of the cavities, leading to an extensive mucous layer on top of a thin intestine-like epithelium (H, 10-wk-old epithelium).

differentiation. This finding, in turn, suggests that loss of *Klf4* expression in the variants is not a consequence of attenuated terminal epidermal differentiation, but rather may be a direct effect of Smad-mediated transcriptional control.

Loss of the epidermal differentiation potential was accompanied by the occurrence of a distinct alternative epithelial phenotype. Both variants expressed a marker profile that was best defined as mucous/intestinal-type epithelial differentiation. This stable phenotypic switch could only be reverted when treating the H-Smad7 epithelia with Smad7 antisense oligonucleotides and thereby reducing the level of Smad7. This treatment resulted in reexpression of epidermal and suppression of mucous/intestinal differentiation markers substantiating that the phenotypic switch indeed depended on active TGF $\beta$ /Smad signaling.

The two genetic variants exhibited a similar, although not identical, differentiation phenotype. Both displayed induction of a mucous/intestinal-type differentiation, however, the H-S234KD epithelia still coexpressed the basic epidermal differentiation set ("early" epidermal differentiation markers), whereas overexpression of Smad7 seemed to cause a more complete switch by blocking the entire epidermal differentiation program. Unfortunately, a mouse correlate for the H-S234KD cells was not yet described. In the Smad7 transgenic mouse model, however, hair follicle morphogenesis was delayed or even abrogated, whereas sebaceous gland development was significantly accelerated and reinforced (Han *et al.*, 2006). In light of our findings that Smad7 overexpression in human HaCaT keratinocytes resulted in a switch from a cornified squamous (epidermal) to a mucous/intestinal-type differentiation with markers

characteristic for glandular-like differentiation, it is tempting to speculate that high levels of Smad7 in mouse skin actually promoted sebaceous differentiation at the expense of hair follicle differentiation.

Concerning the mechanisms of this differentiation programming, it was shown that Smad7 negatively interacts with  $\beta$ -catenin by degrading it and thereby antagonizing Wnt/ $\beta$ -catenin signaling (Han *et al.*, 2006). As the Wnt-pathway is a substantial activator of hair follicle morphogenesis (Ito *et al.*, 2007), the observed severe disturbance of hair follicle morphology in mice with Smad7-overexpression in skin was expected. For the IFE, the role of Wnt signaling is still elusive (Watt and Collins, 2008). Nevertheless, two of our observations indicate a potential role for Smad7 in degrading  $\beta$ -catenin: In 2D cultures of H-Smad7 cells  $\beta$ -catenin became reduced upon TGF $\beta$  treatment (Supplemental Figure S3), and immunostaining of H-Smad7 epithelia revealed a less regular membrane localization of the E-cadherin/ $\beta$ -catenin complex compared with that in epithelia of parental HaCaT cells (Supplemental Figure S4 and unpublished data). In IFE, however, a causal relationship between reduced Wnt/ $\beta$ -catenin signaling and loss of epidermal differentiation is unlikely, which is also suggested by studies specifically addressing the role of Wnt pathway activation in epidermal differentiation (Wischermann, Stark, and Boukamp, unpublished data) and further supported by the fact that a similar nonepidermal phenotype developed through abrogation of Smad2, -3, and -4. Our data suggest that active TGF $\beta$ /Smad signaling is indispensable for epidermal differentiation. Furthermore, because impeding it induces a complex shift to a mucous/intestinal-like differentiation with all specific features including mucous formation, TGF $\beta$ /Smad signaling appears to be the crucial determinant of the terminal differentiation program in the IFE.

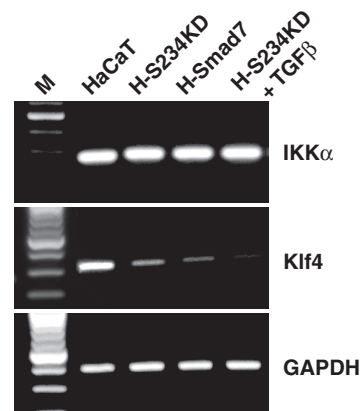


**FIGURE 9:** Involvement of *Klf4* but not *IKK $\alpha$*  in the regulation of epidermal and alternative differentiation programs. RT-PCR analysis was performed from mRNA isolated from epithelia of parental HaCaT cells, two HaCaT variants, and H-S234KD cells treated with TGF $\beta$ . All epithelia were tested for *IKK $\alpha$*  and *Klf4* expression. *GAPDH*, loading control.

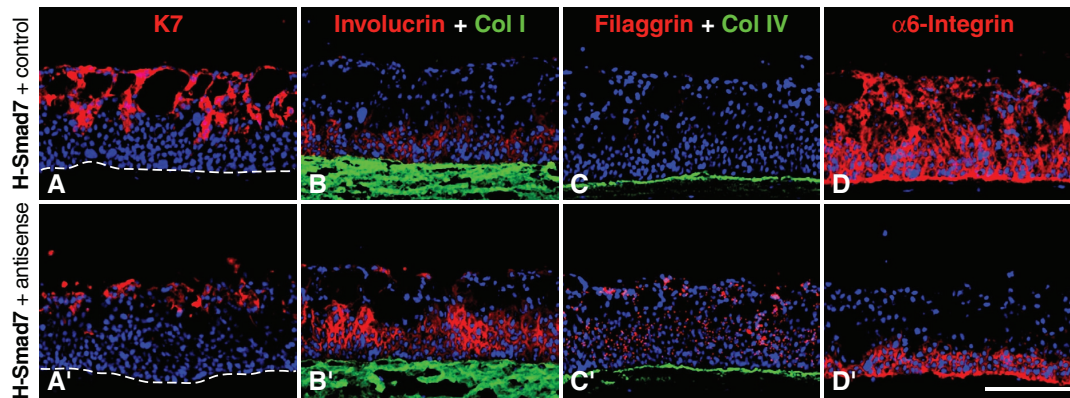


**FIGURE 10:** Extensive reversion of phenotypic abnormalities by counteraction of TGF $\beta$  signaling blockade. Immunofluorescence detection of 4-wk-old OTCs from Smad7 cells grown in the presence of either unrelated oligonucleotides (control, A–D) or Smad7-specific antisense oligonucleotides (antisense, A'–D'). The intestinal keratin K7, which is strongly expressed in the controls (A), is largely absent in oligo-treated cultures (A'). Inversely, the epidermal differentiation marker involucrin largely absent in the control (B) is clearly expressed (B'). Even the "late" epidermal differentiation marker filaggrin, absent in the control (C), is reexpressed in the Smad7-oligonucleotide-treated epithelium (C'). Integrin  $\alpha_6$  expressed throughout the epithelium in the control (D) is largely restricted to the basal layer (D'), indicating phenotypic normalization on smad7 antisense oligonucleotide treatment. All of the previously mentioned proteins are shown in red. Nuclei are counterstained with DAPI (blue), and collagen Type I (col I: B, B') and collagen Type IV (col IV: C, C'), both in green, are marking the dermal equivalent and BM, respectively. The BM in A and A' is demarcated by dashed lines. Nuclei, Hoechst counterstain. Bar = 100  $\mu$ m.

TGF $\beta$  is interconnected with multiple regulatory effectors in an intricate network (Moustakas and Heldin, 2009). Accordingly, it was suggested that TGF $\beta$  modulates differentiation through the regulation of Id proteins by interfering with *prodifferentiation* basic helix-loop-helix transcription factors (Tang *et al.*, 2007). HaCaT keratinocytes overexpressing Id 1 showed hyperproliferation in OTCs, although still restricted to the basal layer, and an abnormal (patchy) distribution of the "late" epidermal differentiation markers (Rotzer *et al.*, 2006). This underlines the contribution of Id-1 in differentiation control. The phenotypic differences presented here, however, question a major role of Id-1 in the TGF $\beta$ -dependent scenario. In contrast, overexpression of cyclin D1 caused a comparable abnormal distribution of proliferation throughout the entire epithelium (Burnworth *et al.*, 2006). Notably, cyclin D1 expression was not altered by Smad pathway interference, as it increased upon TGF $\beta$  treatment in control HaCaT cells as well as H-Smad7 cells, arguing against a Smad pathway-dependent mechanism as the only initiator of disturbed homeostasis and anomalous suprabasal proliferation. Consequently, an additional nonSmad pathway-dependent regulation may elicit this particular proliferation phenotype.

In summary, we used HaCaT cells that were modulated in their TGF $\beta$  signaling as surrogates of human interfollicular epidermal keratinocytes in an *in vivo*-like experimental approach (OTC), and our results contribute toward unraveling further the multiple roles of TGF $\beta$  in epidermal growth and differentiation. We show for the first time that both the observed TGF $\beta$ -dependent growth suppression and "in vivo"-dependent human epidermal tissue homeostasis are regulated in a spatiotemporal manner by the interplay of Smad-dependent and independent pathway controls. In contrast, Smad signaling is indispensable for terminal epidermal differentiation and is central in the decision between alternative epithelial differentiation programs.

## MATERIALS AND METHODS

### Cell cultures and transfection

HaCaT cells and H-S234KD cells expressing small interfering RNA against Smad2, -3, and -4 (Jazag *et al.*, 2005) were maintained in

DMEM (Lonza, formerly Cambrex, Verviers, Belgium), supplemented with 5% fetal calf serum (FCS) (Biochrom, Berlin, Germany). H-Smad7 cells were generated by transfecting HaCaT cells with a pcDNA3 expression vector containing the murine Smad7 cDNA with a Flag-tag at its N terminus (Nakao *et al.*, 1997). Transfections were performed using Effectene Transfection Reagent (Qiagen, Hilden, Germany) and transfectants selected in DMEM/5% FCS containing G418 at 800  $\mu$ g/ml. Two clones overexpressing Flag-Smad7 were selected for further analysis, one constitutively expressing high amounts of Flag-Smad7 and the other showing increased amounts upon TGF $\beta$ 1 treatment (Supplemental Figure S1).

OTCs, using Type I collagen gels with integrated fibroblast as dermal equivalents, were performed as described (Schoop *et al.*, 1999). HaCaT cells or the transgenic variants were seeded on top of the collagen gels and, after 24 h of submersed cultivation, the cultures were air lifted. Medium was changed every second day. Where indicated, 5 ng/ml were added to the culture medium with the air lift, and medium including TGF $\beta$ 1 was renewed every second day. Long-term OTCs were performed as described (Stark *et al.*, 2004). Three parallel cultures were set up for each time point and treatment regimen, and all experiments were repeated at least twice.

To determine the contribution of growth factors, collagen Type I-OTCs were performed with and without integrated fibroblast (Schoop *et al.*, 1999). H-Smad7 cells were seeded on top, and the cultures were cultivated in plain medium or medium with TGF $\beta$  (2 ng/ml) supplemented or not with a neutralizing antibody against EGFR (2  $\mu$ g/ml) throughout the entire cultivation time or a neutralizing antibody against KGF (2  $\mu$ g/ml until day 9 and 1  $\mu$ g/ml until day 21). The medium was renewed every second day.

To investigate the role of TGF $\beta$ , collagen Type I-OTCs were performed with HaCaT and H-Smad7 cells and treated with plain medium, TGF $\beta$  (2 ng/ml), TGF $\beta$  (2 ng/ml plus TGF $\beta$ -neutralizing antibody at 5  $\mu$ g/ml), TGF $\beta$ -neutralizing antibody (5  $\mu$ g/ml) only, and an irrelevant control antibody (5  $\mu$ g/ml). The medium was renewed every other day, and the cultures were terminated at day 16.

For H-Smad7 antisense oligonucleotide experiments, the OTCs were prepared as described earlier in text and treated topically with

6  $\mu$ M oligonucleotides (diluted in 100  $\mu$ l of culture medium per OTC) by using either antisense Smad7 (1: TGA GGT AGA TCA TAG AAG) and (2: GCA CCA GTG TGA CC) or control oligonucleotides (1: ACT ACT ACA CTA GAC TAC) and (2: ACC GAC CGA CGT GT) (all designed, synthesized, and high-performance liquid chromatography-purified by Biognostik, Goettingen, Germany). The oligonucleotides were applied in medium on top of the epithelium every other day for 4 wk starting 24 h after plating the keratinocytes onto the dermal equivalent. In addition, untreated OTCs and OTCs topically treated only with medium were used as controls. Two series of experiments with three parallel cultures for each time point for two independent H-Smad7 clones were performed.

For the nuclear translocation assay, the cells were seeded on glass slides at a density of  $5 \times 10^5$  cells. After 24 h, TGF  $\beta$ 1 at 5 ng/ml was applied for 90 min, and then the cells were fixed for further analysis.

Growth curves were performed by seeding  $2 \times 10^5$  cells in 6-cm culture dishes followed by cultivation for 48 h. Thereafter, the cells were counted every 24 h for 4 consecutive days using a CASY cell counter (Schärfe System, Reutlingen, Germany). TGF $\beta$ 1 (5 ng/ml) was added 24 h after plating, and fresh TGF $\beta$ 1 was added with each medium change every second day. Each time point and treatment was analyzed in duplicate, and one representative experiment of three repetitions is shown.

### Histological analysis

OTCs were fixed in 3.7% formaldehyde (in phosphate-buffered saline [PBS], pH 7.4) for 24 h, embedded in 3% agar (in PBS), and additionally fixed for 24 h. Thereafter, they were processed for routine histology following standard protocols. Five-micrometer sections were stained with hematoxylin and eosin, analyzed with an Olympus AX-70 microscope and recorded with a CCD camera (Color View, Olympus, Hamburg, Germany) applying Analysis Pro 6.0 software (Soft Imaging Systems, Muenster, Germany).

### Detection of mucous substances

Alcian blue staining was performed on paraffin-embedded sections of OTCs after removal of paraffin and rehydration. The sections were acidified (3% acetic acid, 5 min), incubated in Alcian blue solution (1 g of Alcian blue, 3 ml of glacial acetic acid, 97 ml of distilled H<sub>2</sub>O, 30 min), and counterstained with Nuclear fast red (0.2 g of Nuclear fast red, 15 mM aluminum phosphate, 200 ml of H<sub>2</sub>O, 3 min). The sections were rinsed in water, dehydrated in graded ethanol solutions transferred into xylene, and then mounted in Eukitt.

For PAS staining, the sections were oxidized in Periodic acid (0.6%, 10 min) and stained with Schiff's reagent (5 g of basic Fuchsin in 135 ml of 1M HCl, 5 g of potassium disulfide in 200 ml of H<sub>2</sub>O, 5–10 min), followed by immersion in disulfide water and running tap water. Nuclei were counterstained with hematoxylin, differentiated in acidic ethanol solution (70% ethanol containing 2.5% HCl), dehydrated, and mounted.

The reagents for Accustain mucicarmine stain were obtained from Sigma-Aldrich (St. Louis, MO) and applied according to the manufacturer's instructions (procedure no. HT30).

### Indirect immunofluorescence microscopy

OTCs were embedded in Tissue Tek (Sakura Finetek, Zoeterwoude, The Netherlands) and frozen in the gas phase of liquid nitrogen. Cryostat sections (5  $\mu$ m) or cells grown on slides were fixed in 80% methanol at 4°C and 100% acetone at –20°C and air-dried. After rehydration in PBS and blocking with 5% (wt/vol) bovine serum albu-

min in PBS supplemented with 0.02% (wt/vol) sodium azide, specimens were treated with the respective primary antibodies for 2 h at room temperature. Generally, two primary antibodies of the respective species of the primary antibodies were combined on the same section. After washing in PBS, the sections were incubated with an appropriate combination of fluorochrome-conjugated secondary antibodies for 1 h at room temperature. The nuclei were counterstained with Hoechst dye 33258. Slides were rinsed in PBS and mounted in Permafluor. Images were recorded as described earlier in text.

### Western blot analysis

Western blot analyses were performed as described previously (Cerezo *et al.*, 2002). Cell pellets were lysed in RIPA buffer, protein concentrations determined by Bradford staining (Bio-Rad Laboratories, Munich, Germany), and 30  $\mu$ g of total protein was separated by SDS-PAGE using a 12% polyacrylamide gel. For antibody detection, the SuperSignal West Pico chemiluminescence detection system (Pierce/Perbio Science, Bonn, Germany) was used. Ponceau-stained nitrocellulose membranes served as controls for loading and transfer efficiency.

### Antibodies and reagents

Recombinant human TGF $\beta$ 1 (R&D Systems, Wiesbaden, Germany) was dissolved in 4 mM HCl and diluted to a stock concentration of 2  $\mu$ g/ml. Neutralizing antibodies were used for the EGFR (humanized mouse monoclonal anti-EGFR antibody, Cetuximab; Merck, Darmstadt, Germany), the KGF (mouse monoclonal anti-KGF/FGF-7 antibody), TGF $\beta$  (mouse monoclonal anti TGF $\beta$ 1, -2, -3 antibody), and mouse monoclonal anti-pox virus-chemokine inhibitor (CCI) antibody was used as isotopic control antibody (all three from R&D Systems, Wiesbaden, Germany).

Primary antibodies for immunoblotting were as follows: rabbit polyclonal antibodies against phospho-Smad2 (Persson *et al.*, 1998), phospho-Smad3 (Cell Signaling Technology/New England Biolabs, Frankfurt, Germany), cyclin D1 (ab31450; Abcam, Cambridge, UK), p15 (C-20), p21(C-19), and CDK4 (H-22), the mouse monoclonal antibodies against PAI-1 (C-9) as well as the goat polyclonal antibodies against Smad2/3 (N-19) and Smad7 (N-19) (all obtained from Santa Cruz Biotechnology, Heidelberg, Germany).

Primary antibodies for indirect immunofluorescence were as follows: rabbit polyclonal antibodies against Ki67 (Abcam), loricrin (provided by D. Hohl, CHUV, Lausanne, Switzerland), collagen Type IV (Heyl, Berlin, Germany), collagen I (US Biological, Swampscott, MA), vitronectin (Biomol, Hamburg, Germany), and Dsg2 (Progen, Heidelberg, Germany); mouse monoclonal antibodies against keratins K1/K10 (clone 8.60), E-cadherin (clone 5H9), and keratin K19 (clone Ks19.1); Dsg1/2 (clone DG3/10), Dsg1 (clone P124), and Dsg3 (G194) (all obtained from Progen, Heidelberg, Germany); involucrin (clone SY5) and keratin K4 (clone 6B10) (both obtained from Sigma, Taufkirchen, Germany); transglutaminase-1 and filaggrin (both obtained from Cell Systems, St. Katharinen, Germany); filaggrin (clone FLG01; Thermo Fisher Scientific, Fremont, CA) and keratin K7 (GE Healthcare, formerly Amersham, Munich, Germany); rat monoclonal antibodies against integrin  $\alpha$ 6 and  $\beta$ 1 (both obtained from Millipore, formerly Chemicon, Schwalbach, Germany); and guinea pig polyclonal antibodies against keratins K13, K2, K5, K14, cingulin, vimentin, and Dsg4 (all obtained from Progen).

The secondary antibodies used for immunoblotting were peroxidase-conjugated donkey anti-mouse-, anti-rabbit-, and anti-goat immunoglobulin (IgG) (H+L) (all obtained from Dianova, Hamburg, Germany) and, for immunofluorescence, goat anti-mouse and

anti-rabbit IgG (H+L) Alexa Fluor 488 (both obtained from Molecular Probes/Invitrogen, Karlsruhe, Germany), donkey anti-mouse-, anti-rabbit-, anti-goat-, and anti-guinea pig IgG (H+L) Cy3 (Dianova). Nuclei were counterstained with Hoechst dye 33258 (Sigma, Taufkirchen, Germany).

### In situ hybridization

For in situ hybridization, a 371 bp cDNA probe of the Smad7 coding 5'-end (nt pos. 40–410) was generated by PCR and cloned into pCR2.1 vector. This system allows the synthesis of a specific probe by using T7-RNA polymerase (Roche, Mannheim, Germany). As a positive control, a specific probe of the keratin K14 3'-coding region of 380 bp was used.

Labeling of the cRNA probes and the in situ hybridization procedure were performed essentially as described (Langbein *et al.*, 2004). Briefly, for the Dig-labeling of the cRNA probe, the DIG-RNA labeling Kit (Roche) was used following the instructions of the manufacturer. After denaturation of the sections at 90°C, prehybridization with 2× saline-sodium citrate/50% formamide and hybridization with the probe was done at 42°C overnight. Stringent washing steps were done at 50°C including one RNaseA digestion step. For detection, the bound probe was labeled with an alkaline phosphatase-labeled goat anti-Dig antibody (1:300 vol; Roche). For blocking internal tissue phosphatases, sections were treated with levamisole (2 mg/10 ml) for 30 min. For the color substrate reaction of the phosphatase, Nitroblue tetrazolium chloride/5-bromo-4-chloro-3-indolyl phosphate substrate tablets (Roche) were used. Positive (K14) and negative (hybridization buffer; sense probes) controls were performed.

### RNA isolation, RT-PCR, and quantitative RT-PCR analysis

Total RNA was isolated from the epithelia (OTCs) separated from the dermal equivalent. RNA was extracted using RNeasy according to the manufacturer's instructions (Qiagen). One microgram of total RNA was reversely transcribed to cDNA (Omniscript; Qiagen) as described previously (Cerezo *et al.*, 2003). The cDNA template was used in a PCR with the primers for IKK $\alpha$ : forward primer 1603–1622, AAAGGCCATCCAATGCTG, and reverse primer 1874–1855, GACCAAACAGCTCCTTGAGC, with a PCR product length of 272 base pairs; for Klf4, forward primer 1387–1406, CGCTCCATTACAAGAGCTC, and reverse primer 1726–1707, ATGTGTAAGGC-GAGGTGGTC, with a PCR product length of 340 base pairs. For mucin 4: forward primer CTT CAC CTC CCC ACT CTT CA, and reverse primer TGT AGC CCC CGT TGT TTG T, mucin 13: forward primer ATA ATC ACC GCT TCA TCT CCA, and reverse primer GTC ATC AGC ACG CAT TTC A, and Gcnt3: forward primer TTC AAA GAG GCG GTC AAA GCA, and reverse primer TGT CGT ACT TGG GGT GGT TGG. PCR conditions for 25 cycles for Klf4, 30 cycles for IKK $\alpha$ , 23 cycles for GAPDH, and 30 cycles for mucin 4, mucin 13, and Gcnt3 were as follows: denaturation for 2 min at 95°C, 15 s at 94°C, 30 s at 60°C, 30 s at 72°C, and final extension for 10 min at 72°C.

Quantitative RT-PCR (qRT-PCR) was performed in a capillary-based LightCycler 1.2 according to the manufacturer's instructions. Each reaction consists of a 15- $\mu$ l mix in nuclease-free water containing 4  $\mu$ l of LightCyclerTaqMan master, 0.2  $\mu$ M Smad3 forward (GTCTGCAAGATCCCACCAG) and reverse (AGCCCTGGTTGACCGACT) primers, and 0.1  $\mu$ M UPL-probe #79 (Universal ProbeLibrary; Roche). This mix was then pipetted into the capillaries, and 50–200 ng of cDNA in 5  $\mu$ l of RNase-free water was added. A negative control containing water instead of cDNA was run for each primer pair and reaction. After a preincubation at 95°C for 10 min, the amplification was carried out in 45 cycles, each consisting of

heating for 10 s at 95°C and annealing for 30 s at 60°C. Fluorescence was measured at 530 nm after each cycle and monitored by LightCycler software (version 3.5). The reaction was finished with a cooling step at 40°C for 10 s. For relative quantification, the gene of interest and a housekeeping gene (e.g., GAPDH) were analyzed for each control and sample. Using the software and the algorithm Second Derivative Maximum, the crossing point of each gene in a given sample was calculated identifying the cycle number at which the fluorescence signal rises above background fluorescence. With these crossing point values, the ratio of relative mRNA expression of control versus sample normalized to the housekeeping gene was calculated. Controls were always set to 1. To verify the quality of the primer/probe combination and the efficiency of the PCR, standard curves were performed for each test.

### ACKNOWLEDGMENTS

We thank Angelika Krischke and Iris Martin for excellent technical assistance and Berit Falkowska-Hansen for providing a micrograph of a HaCaT long-term OTC. We also thank Jennifer Pietenpol and Christopher Barton, Vanderbilt University, Nashville, TN, and Sabine Werner, ETH Zürich, Switzerland, for critically reading; and Angelika Lampe for her help in preparing and Yetunde Odunsi for orthographically correcting the manuscript. We wish to extend our thanks to Peter ten Dijke, Department of Molecular Cell Biology and Center for Biomedical Genetics, Leiden University Medical Center, The Netherlands, for kindly providing us with the Smad7 construct and Fumihiko Kanai, Department of Gastroenterology, University of Tokyo, Tokyo, Japan, for kindly providing us with the H-S234KD cells. This work was in part funded by EU-WOUND, Baden-Württemberg Stiftung, Krebshilfe-Tumorstammzellverbund, BMBF Medsys (0315401A), and (SFB 835) (all to P.B.) and by the Friedrich Sander Stiftung (2007.133.1 to L.L.).

### REFERENCES

- Boehnke K, Mirancea N, Pavesio A, Fusenig NE, Boukamp P, Stark HJ (2007). Effects of fibroblasts and microenvironment on epidermal regeneration and tissue function in long-term skin equivalents. *Eur J Cell Biol* 86, 731–746.
- Brown KA, Pietenpol JA, Moses HL (2007). A tale of two proteins: differential roles and regulation of Smad2 and Smad3 in TGF- $\beta$  signaling. *J Cell Biochem* 101, 9–33.
- Burnworth B, Popp S, Stark HJ, Steinkraus V, Brocker EB, Hartschuh W, Birek C, Boukamp P (2006). Gain of 11q/cyclin D1 overexpression is an essential early step in skin cancer development and causes abnormal tissue organization and differentiation. *Oncogene* 25, 4399–4412.
- Cerezo A, Kalthoff H, Schuermann M, Schafer B, Boukamp P (2002). Dual regulation of telomerase activity through c-Myc-dependent inhibition and alternative splicing of hTERT. *J Cell Sci* 115, 1305–1312.
- Cerezo A, Stark HJ, Moshir S, Boukamp P (2003). Constitutive overexpression of human telomerase reverse transcriptase but not c-myc blocks terminal differentiation in human HaCaT skin keratinocytes. *J Invest Dermatol* 121, 110–119.
- Chen X, Whitney EM, Gao SY, Yang VW (2003). Transcriptional profiling of Kruppel-like factor 4 reveals a function in cell cycle regulation and epithelial differentiation. *J Mol Biol* 326, 665–677.
- Contard P, Jacobs L, Perlish JS, Fleischmajer R (1993). Collagen fibrillogenesis in a three-dimensional fibroblast cell culture system. *Cell Tissue Res* 273, 571–575.
- Datta PK, Blake MC, Moses HL (2000). Regulation of plasminogen activator inhibitor-1 expression by transforming growth factor- $\beta$ -induced physical and functional interactions between smads and Sp1. *J Biol Chem* 275, 40014–40019.
- De Robertis EM, Kuroda H (2004). Dorsal-ventral patterning and neural induction in *Xenopus* embryos. *Annu Rev Cell Dev Biol* 20, 285–308.
- Dennler S, Itoh S, Vivien D, ten Dijke P, Huet S, Gauthier JM (1998). Direct binding of Smad3 and Smad4 to critical TGF- $\beta$ -inducible elements in the promoter of human plasminogen activator inhibitor-type 1 gene. *EMBO J* 17, 3091–3100.

- Descargues P, Sil AK, Sano Y, Korchynskiy O, Han G, Owens P, Wang XJ, Karin M (2008). IKK $\alpha$  is a critical coregulator of a Smad4-independent TGF $\beta$ -Smad2/3 signaling pathway that controls keratinocyte differentiation. *Proc Natl Acad Sci USA* 105, 2487–2492.
- El Ghalbzouri A, Lamme E, Ponc M (2002). Crucial role of fibroblasts in regulating epidermal morphogenesis. *Cell Tissue Res* 310, 189–199.
- Fusenig NE (1994). Epithelial-mesenchymal interactions regulate keratinocyte growth and differentiation in vitro. In: *The Keratinocyte Handbook*, ed. I Leigh, B Lane, and F Watt, Cambridge, UK: Cambridge University Press, 71–94.
- Green KJ, Simpson CL (2007). Desmosomes: new perspectives on a classic. *J Invest Dermatol* 127, 2499–2515.
- Halder SK, Beauchamp RD, Datta PK (2005). Smad7 induces tumorigenicity by blocking TGF- $\beta$ -induced growth inhibition and apoptosis. *Exp Cell Res* 307, 231–246.
- Han G et al. (2006). Smad7-induced beta-catenin degradation alters epidermal appendage development. *Dev Cell* 11, 301–312.
- Heldin CH, Landstrom M, Moustakas A (2009). Mechanism of TGF- $\beta$  signaling to growth arrest, apoptosis, and epithelial-mesenchymal transition. *Curr Opin Cell Biol* 21, 166–176.
- Hua X, Miller ZA, Wu G, Shi Y, Lodish HF (1999). Specificity in transforming growth factor beta-induced transcription of the plasminogen activator inhibitor-1 gene: interactions of promoter DNA, transcription factor muE3, and Smad proteins. *Proc Natl Acad Sci USA* 96, 13130–13135.
- Hunter T, Pines J (1994). Cyclins and cancer. II: Cyclin D and CDK inhibitors come of age. *Cell* 79, 573–582.
- Inman GJ, Nicolas FJ, Hill CS (2002). Nucleocytoplasmic shuttling of Smads 2, 3, and 4 permits sensing of TGF- $\beta$  receptor activity. *Mol Cell* 10, 283–294.
- Ito M, Yang Z, Andl T, Cui C, Kim N, Millar SE, Cotsarelis G (2007). Wnt-dependent de novo hair follicle regeneration in adult mouse skin after wounding. *Nature* 447, 316–320.
- Jazag A et al. (2005). Single small-interfering RNA expression vector for silencing multiple transforming growth factor-beta pathway components. *Nucleic Acids Res* 33, e131.
- Langbein L, Rogers MA, Praetzel S, Aoki N, Winter H, Schweizer J (2002). A novel epithelial keratin, hK6irs1, is expressed differentially in all layers of the inner root sheath, including specialized Huxley cells (Flugelzellen) of the human hair follicle. *J Invest Dermatol* 118, 789–799.
- Langbein L, Rogers MA, Praetzel S, Winter H, Schweizer J (2003). K6irs1, K6irs2, K6irs3, and K6irs4 represent the inner-root-sheath-specific type II epithelial keratins of the human hair follicle. *J Invest Dermatol* 120, 512–522.
- Langbein L, Spring H, Rogers MA, Praetzel S, Schweizer J (2004). Hair keratins and hair follicle-specific epithelial keratins. *Methods Cell Biol* 78, 413–451.
- Li RW, Li C, Elsasser TH, Liu G, Garrett WM, Gasbarre LC (2009). Mucin biosynthesis in the bovine goblet cell induced by *Cooperia oncophora* infection. *Vet Parasitol* 165, 281–289.
- Maas-Szabowski N, Shimotoyodome A, Fusenig NE (1999). Keratinocyte growth regulation in fibroblast cocultures via a double paracrine mechanism. *J Cell Sci* 112, Pt 121843–1853.
- Maas-Szabowski N, Stark HJ, Fusenig NE (2000). Keratinocyte growth regulation in defined organotypic cultures through IL-1-induced keratinocyte growth factor expression in resting fibroblasts. *J Invest Dermatol* 114, 1075–1084.
- Moll R, Divo M, Langbein L (2008). The human keratins: biology and pathology. *Histochem Cell Biol* 129, 705–733.
- Moustakas A, Heldin CH (2009). The regulation of TGF $\beta$  signal transduction. *Development* 136, 3699–3714.
- Muffler S, Stark HJ, Amoros M, Falkowska-Hansen B, Boehnke K, Buhring HJ, Marme A, Bickenbach JR, Boukamp P (2008). A stable niche supports long-term maintenance of human epidermal stem cells in organotypic cultures. *Stem Cells* 26, 2506–2515.
- Nakao A et al. (1997). Identification of Smad7, a TGF $\beta$ -inducible antagonist of TGF- $\beta$  signaling. *Nature* 389, 631–635.
- Owens P, Han G, Li AG, Wang X (2008). The role of Smads in skin development. *J Invest Dermatol* 128, 783–790.
- Patel V, Jakus J, Harris CM, Ensley JF, Robbins KC, Yeudall WA (1997). Altered expression and activity of G1/S cyclins and cyclin-dependent kinases characterize squamous cell carcinomas of the head and neck. *Int J Cancer* 73, 551–555.
- Persson U, Izumi H, Souchelnytskyi S, Itoh S, Grimsby S, Engstrom U, Heldin CH, Funahashi K, ten Dijke P (1998). The L45 loop in type I receptors for TGF- $\beta$  family members is a critical determinant in specifying Smad isoform activation. *FEBS Lett* 434, 83–87.
- Providence KM, Kutz SM, Staiano-Coico L, Higgins PJ (2000). PAI-1 gene expression is regionally induced in wounded epithelial cell monolayers and required for injury repair. *J Cell Physiol* 182, 269–280.
- Rotzer D, Krampert M, Sulyok S, Braun S, Stark HJ, Boukamp P, Werner S (2006). Id proteins: novel targets of activin action, which regulate epidermal homeostasis. *Oncogene* 25, 2070–2081.
- Schafer M, Werner S (2008). Cancer as an overhealing wound: an old hypothesis revisited. *Nat Rev Mol Cell Biol* 9, 628–638.
- Schoop VM, Mirancea N, Fusenig NE (1999). Epidermal organization and differentiation of HaCaT keratinocytes in organotypic coculture with human dermal fibroblasts. *J Invest Dermatol* 112, 343–353.
- Segre JA, Bauer C, Fuchs E (1999). Klf4 is a transcription factor required for establishing the barrier function of the skin. *Nat Genet* 22, 356–360.
- Shirakata Y (2010). Regulation of epidermal keratinocytes by growth factors. *J Dermatol Sci* 59, 73–80.
- Smola H, Stark HJ, Thiekotter G, Mirancea N, Krieg T, Fusenig NE (1998). Dynamics of basement membrane formation by keratinocyte-fibroblast interactions in organotypic skin culture. *Exp Cell Res* 239, 399–410.
- Song CZ, Siok TE, Gelehrter TD (1998). Smad4/DPC4 and Smad3 mediate transforming growth factor-beta (TGF- $\beta$ ) signaling through direct binding to a novel TGF- $\beta$ -responsive element in the human plasminogen activator inhibitor-1 promoter. *J Biol Chem* 273, 29287–29290.
- Stark HJ, Boehnke K, Mirancea N, Willhauck MJ, Pavesio A, Fusenig NE, Boukamp P (2006). Epidermal homeostasis in long-term scaffold-enforced skin equivalents. *J Invest Dermatol Symp Proc* 11, 93–105.
- Stark HJ, Willhauck MJ, Mirancea N, Boehnke K, Nord I, Breitkreutz D, Pavesio A, Boukamp P, Fusenig NE (2004). Authentic fibroblast matrix in dermal equivalents normalises epidermal histogenesis and dermoepidermal junction in organotypic coculture. *Eur J Cell Biol* 83, 631–645.
- Szabowski A, Maas-Szabowski N, Andrecht S, Kolbus A, Schorpp-Kistner M, Fusenig NE, Angel P (2000). c-Jun and JunB antagonistically control cytokine-regulated mesenchymal-epidermal interaction in skin. *Cell* 103, 745–755.
- Tang B et al. (2007). Transforming growth factor-beta can suppress tumorigenesis through effects on the putative cancer stem or early progenitor cell and committed progeny in a breast cancer xenograft model. *Cancer Res* 67, 8643–8652.
- Watabe T, Miyazono K (2009). Roles of TGF- $\beta$  family signaling in stem cell renewal and differentiation. *Cell Res* 19, 103–115.
- Watt FM, Collins CA (2008). Role of beta-catenin in epidermal stem cell expansion, lineage selection, and cancer. *Cold Spring Harb Symp Quant Biol* 73, 503–512.